EUROPHYSICS LETTERS 15 September 2002

Europhys. Lett., **59** (6), pp. 827–833 (2002)

Instability of a confined jet impinging on a water/air free surface

G. Bouchet[1], E. Climent[1] and A. Maurel[2]

[1] *Institut de Mécanique des Fluides et des Solides de Strasbourg UMR CNRS/ULP 7507 - 2 rue Boussingault, 67000 Strasbourg, France*
[2] *Laboratoire Ondes et Acoustique, UMR CNRS 7587, ESPCI 10 rue Vauquelin, 75231 Paris Cedex 05, France*

(received 25 April 2002; accepted in final form 20 June 2002)

PACS. 47.15.Rq – Laminar flows in cavities.
PACS. 47.54.+r – Pattern selection; pattern formation.
PACS. 47.20.-k – Hydrodynamic stability.

Abstract. – Self-sustained oscillations in sinuous mode occur when a water jet impinges from below on a water/air free surface. Confined jet instability is experimentally investigated by image processing and velocity measurements. Despite small deformations of the surface, dynamic response of the jet provides unusual behaviour with comparable configurations (hole-tone, jet edge ...). The central feature is a bounded evolution of the oscillation frequency. Modal transitions are observed when physical parameters are varied. Each frequency jump is related to wavelength modification of the spatial pattern. Atypical evolution of the predominant length scale has to be connected to strong coupling with the weak deformations induced by the impinging jet on the free surface.

Introduction. – Self-induced oscillations are present in various physical situations such as flows in cavity-type geometry. This is the case of jet impingement on obstacles, for example the jet-edge extensively described in the literature since [1], the hole-tone or sudden expansion configurations and many wind instruments (a review is given by [2]). Common experiences in air suggest the production of discrete tones by these instruments related to frequency selection. Such a behaviour of oscillators illustrates that confined jets are able to develop robust dynamics, as opposed to free jets belonging to the so-called noise amplifiers that are unable to select a well-defined frequency [3]. It is widely accepted in the literature that dynamic response modifications are connected to the existence of a feedback loop between the jet nozzle and the obstacle. Initial flow disturbances grow while being advected and interact with the impingement point. The feedback loop induces forcing on the inlet flow resulting in a periodic cycle. The physical nature of this feedback could be hydrodynamical [4, 5] or acoustical for compressible flows [6]. As jet impingement on a free surface belongs to self-sustained oscillator configurations, in the presented paper we are interested in the case of a vertical water jet impinging from below on a water/air free interface, known as a "submerged fountain". Our configuration of impinging jet can be related to the study presented in [7]. Viscous liquid jet propagating in liquid environment experiences buckling or folding deformations. Due to

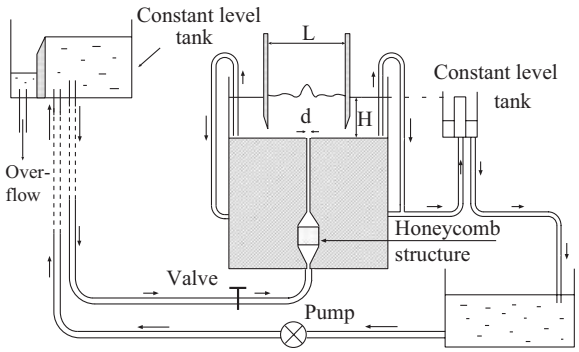

Fig. 1 – Experimental set-up: $d = 10$ mm; $L = 100$–700 mm; $H = 20$–300 mm; the length of the channel between the honeycomb structure and the jet nozzle is equal to $45d$.

negative buoyancy force experienced at the impinged interface, the liquid jet is compressed as a slender solid column. The study of such systems is a natural extension of previous studies on jet and rigid boundary interactions [5]. Fluid-resonant oscillations were already observed when elastic boundaries are impinged by shear layers [8]. Also, this study is connected to many engineering devices such as those used in refuelling where a water jet impinges on a residual layer of fuel [9]. In this latter case, we expect that the feedback loop between the impingement point and the jet nozzle could be affected by possible interface deformations. Complex coupling phenomena could occur between jet and interface dynamics. Former studies were devoted to the analysis of surface oscillations [10, 11] or phase coupling of a network of vertical jets [12].

In the present paper we propose the investigation of the instabilities of the jet core itself and the coupling with surface deformations. We have performed simultaneous measurements in the bulk to characterize jet meandering and at the free surface to study the bump oscillation. As will be described, two types of instabilities have been identified by previous studies but both of them exist in the "submerged fountain". The paper is organized as follows. In the first section, the experimental set-up is described. The second section is devoted to the collection of experimental data obtained on the jet instability. In the latter section, discussion of the particular nature of the jet response is proposed. Finally, occurrence of a secondary instability is briefly outlined.

Experimental set-up. – The experimental set-up is presented in fig. 1. The cavity is an Altuglas parallelepipedic box 20 mm wide, 700 mm long (spanwise confinement L) and 300 mm high (streamwise confinement H). This is a quasi-2D plane cavity. Both confinements influencing the flow dynamic are independent and adjustable. The nozzle is 10 mm wide (d) and placed at the end of a rectangular channel 400 mm long. The experimental configuration is made up of a gravity-driven water flow using a constant level tank (keeping a constant flow rate) and allowing jet velocities U below 1 $\mathrm{m\,s^{-1}}$ (U is the mean velocity at the jet nozzle). This set-up limits parasitic frequencies that might perturb the flow. A honeycomb structure has been used upstream of the cavity to reduce perturbations. We can notice that, due to the long distance between the honeycomb structure and the cavity inlet, the channel flow is fully developed (transitional or weakly turbulent). The flow rate is regulated with a needle valve and measured by an electromagnetic flowmeter, with an accuracy of 0.5%. The water depth H in the cavity is regulated by a second constant-level tank.

Experimentally, it is difficult to keep H constant when U is varied. Therefore, we proceed to systematic measurements of the cavity height by image processing including a temporal

averaging of the small fluctuations of the water level. Thus, the system resolution for water height measurements is 0.25 mm. Unsteady phenomena are measured in the cavity by a pair of very sensitive hot film sensors used in differential connection, placed on both sides of the jet inlet. The wavelength in the bulk and free surface oscillations are obtained by image processing. Typical frames show an area of interest taken from the scene backlit by a controlled illumination avoiding any artifacts at the surface. The scene is composed of a thin dark line created by the optical properties of the water/air surface and contrasting with a white background. This configuration makes it possible to extract a one-pixel–wide outline from the surface. Extracting the horizontal position of the bump top in each frame generates data sets from which the lateral oscillation frequency is computed by FFT-based spectral analysis with an accuracy of 10^{-3} Hz. The flow pattern oscillation in the volume requires artificial contrast generation, since the jet shows no visible optical effect. The water tank is therefore filled with a black dyed liquid, so that the jet core appears dark on a white background, allowing extraction of contours by image processing (see fig. 4a below).

Results on jet behaviour. – As the jet impinges from below on the horizontal water/air surface, a small bump is observed. Analytical models and experimental data on the deformation of interfaces under jet impact between non-miscible fluids have been proposed by [13,14]. The jet momentum impinging on the surface is mainly transformed by negative buoyancy force acting on the jet above the undisturbed level [9]. Due to the very large radius of curvature, capillary effects should remain weak. Stagnation pressure allows the determination of the surface deflection and an instability criterion is provided for large indentations. In all the situations described in the present paper, the bump height is less than 10 mm. For low values of H (smaller than 4 cm) and whatever jet inlet velocity, no oscillations have been observed. As explained in [15], buckling jet threshold has to be related to viscous compressive forces in the jet core. A minimum threshold length is necessary to compress the jet as a slender solid column. Consequently, below $H = 4$ cm, self-sustained oscillations are impossible. Similar results have been pointed out for buckling of liquid jets both experimentally [16] or theoretically [15]. On the contrary, for a larger depth of water cavity, oscillations with a well-defined frequency are noticeable. A spectral ray with an amplitude of two decades, larger than the ambient noise, is identified as the frequency oscillation in every spectrum. The bump oscillates laterally with an amplitude of a few millimeters. No significant gravity waves develop on the water/air interface. Simultaneous analysis of the surface oscillation by image processing and velocity measurements in the bulk of the cavity provide the same frequency, pointing out that lateral displacement of the bump is only the result of jet meandering. The threshold of jet instability (see fig. 2a) in dimensional parameters exhibits a slight trend of decreasing inlet velocity for H increasing ($H \geq 7$ cm).

Above the threshold, for a fixed value of H, the frequency f of the self-sustained oscillations increases with U. Even for the lowest values of U, initial turbulence in the jet core is present. The transitional or weakly turbulent nature of the channel flow upstream of the jet nozzle has undoubtedly no significance on the studied jet instability (see similar studies [2]). For different heights of the cavity, a similar evolution is obtained: a continuous increase of f with U interrupted by discrete frequency jumps. Because of these discrete decreasing jumps, frequency evolution is bounded between 3 Hz and 5 Hz. Such a behaviour is unexpected for confined jet instability. Usually, frequency jumps occur with an increase of the frequency at each modal transition [2]. Frequency jumps are observed either when H increases for fixed values of U or when U increases for fixed values of H. Typical evolutions are plotted in fig. 2b and fig. 3a. Contrary to the buckling of thin liquid jets [16], we observe a reduction of the oscillation frequency when the impinged surface is moved away. All the results presented were

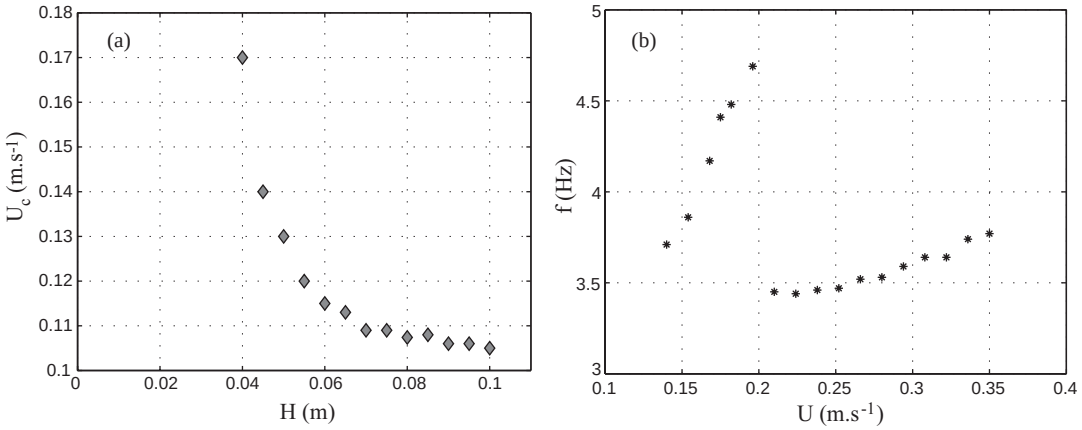

Fig. 2 – (a) Threshold of the jet instability (U_c: critical jet velocity); (b) frequency evolution *vs.* jet velocity ($H = 0.05$ m).

performed with a constant lateral confinement $L = 20$ cm. Indeed, a complete set of experiments with various values of L have demonstrated independent evolution whatever L (less than 1% scattering). Non-dimensionalizing the frequency as a Strouhal number $St = \frac{f.H}{U}$, all the data can be inserted into a single diagram (see fig. 3b). A nearly constant plateau of St indicates that the slope of the linear dependence $f(U)$ is reduced at each frequency jump. It is commonly accepted that frequency discontinuities are related to modal transition, *i.e.* the hydrodynamic system changes in oscillation frequency as the flow field structure is modified. Theoretical reasons for such a modal transition are at the moment unavailable and are probably connected to an energetic budget of each possible coexisting flow.

In figs. 2b and 3a, frequency evolutions are bounded by an upper limit equal to 5 Hz. As a physical explanation of this particular feature we suggest that the system reaches a resonant frequency and selects a new oscillation mode with a lower frequency. The resonance frequency

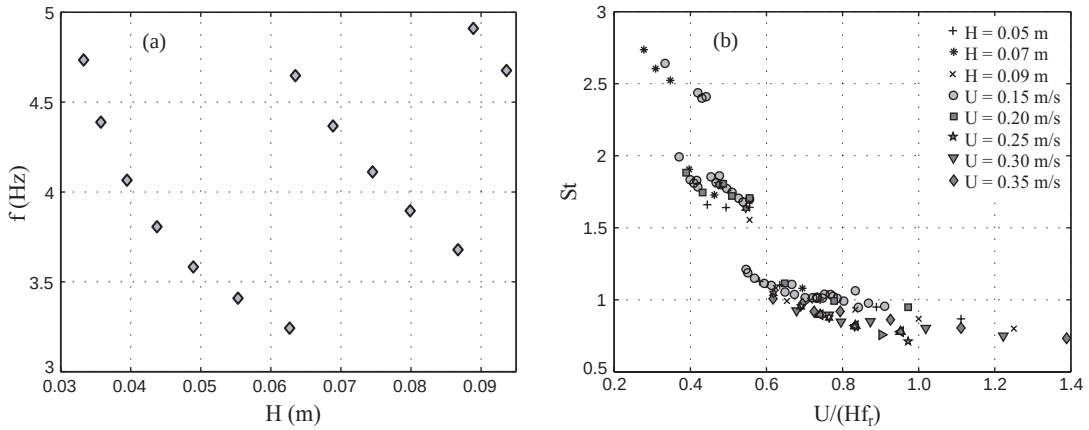

Fig. 3 – (a) Frequency evolution *vs.* impinging distance ($U = 0.15$ m s^{-1}); (b) Strouhal number evolution (symbols are related to different values of H and U).

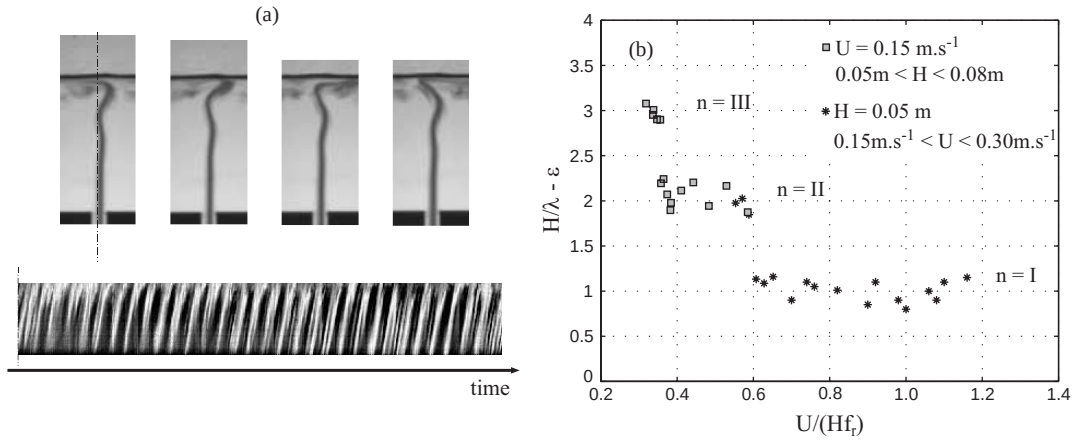

Fig. 4 – (a) Time evolution of the jet meandering and space-time diagram; (b) wavelength number in the jet meandering.

f_r must be related to the flexible nature of the impinged surface (water/air interface). Shear layers on both sides of the jet profile are dynamically unstable. Jet impingement induces small variations of the local height of the cavity by free-surface deformations. Then there follows a feedback forcing on the jet by hydrostatic pressure fluctuations. Resonance is achieved when free surface oscillations are amplified by shear layer instability. The frequency of surface oscillations is correlated to the wavelength of the deformations. Image processing of the bump shape has demonstrated that a typical length scale of surface deformation is controlled by the jet width d and is roughly equal to $3d$. In the deep-water approximation, f_r is related to physical parameters (ρ water density, σ water/air surface tension, g gravity acceleration) by eq. (1), where the wavelength λ_s of the surface deformations is equal to $6d$. This frequency corresponds to surface oscillations induced by gravity and capillary waves,

$$f_\mathrm{r} = \sqrt{\frac{g}{2 \cdot \pi \cdot \lambda_\mathrm{s}} + \frac{2 \cdot \pi \cdot \sigma}{\rho \cdot \lambda_\mathrm{s}^3}} \tag{1}$$

To analyze spatial modification of the flow field, we injected dye to visualize the jet core. As the jet oscillates in a sinuous mode, the meandering motion describes a vertical progressive wave whose characteristics are measured by diagram analysis. This space-time diagram, showing the right or left vertical edge of the jet, is built by copying the updated vertical column of pixels in a custom picture, in which then there appears an oblique pattern of lines (see fig. 4a). The vertical distance between two successive oblique lines equals the jet wavelength, while horizontal time spacing corresponds to the oscillation period. Various configurations have been studied to obtain the relation between H and the jet meandering wavelength λ. As shown in fig. 4b, each frequency jump materialized by a constant Strouhal number in fig. 3b is related to a different wavelength number n, *i.e.* $H = (n + \varepsilon)\lambda$ with $\varepsilon = 0.5$ as an inlet correction [17]. In opposition to the classical dynamics of confined jets [6], the wavelength number n decreases with U for fixed H. This means that the system "selects" larger structures as the inlet velocity is increased. This particular behaviour will be discussed in the next section. Using the same experimental data set, celerity $c = \lambda \cdot f$ exhibits a rather constant ratio with U ($c = 0.7U$). The phase velocity of wave propagation of the sinuous pattern is always related to advective velocity U whatever the selected mode.

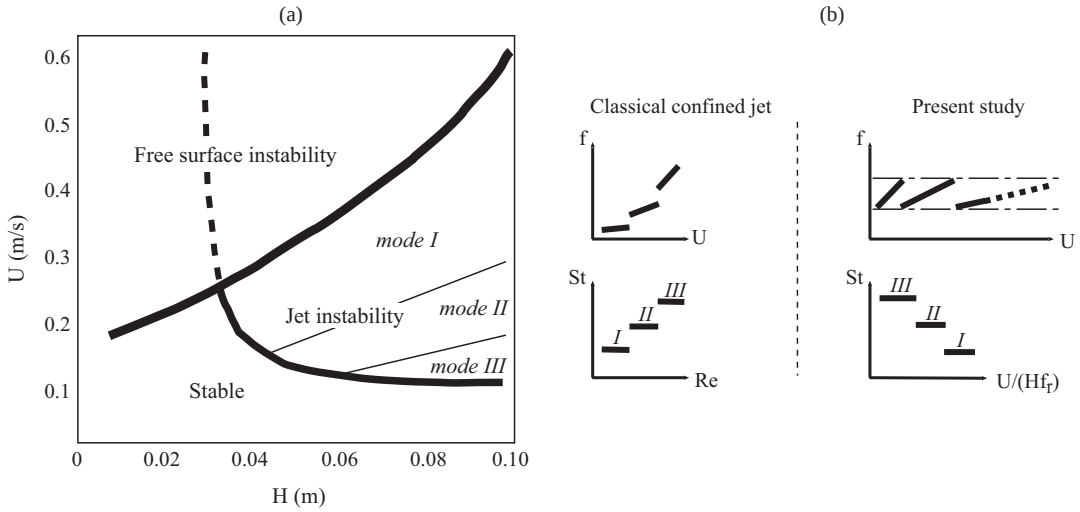

Fig. 5 – (a) Phase diagram; (b) comparison with classical confined jet instabilities [2, 6].

Discussion. – The present section is devoted to point out the atypical response of the jet instability. Indeed the presence of a deforming surface seems to be a crucial point in the flow dynamics. Considering the evolution of frequency with U above the threshold for fixed values of H allows us to construct the schematic phase diagram in terms of physical parameters (see fig. 5); the delimiting lines between flow states are based on a fit of our experimental data. For low velocities, there are no oscillations, and the system is stable. With increasing the flow rate with a constant H, sinuous oscillations of the jet occur with a linear dependence of f with U. Frequency jumps interrupt two linear evolutions with distinct slopes related to constant values of Strouhal number. Connected to these frequency jumps, we have shown by spatial analysis that the jet wavelength varies across the discontinuities of the frequency. We can conclude from fig. 4b that the mode with three wavelengths occurs for a lower inlet velocity than the mode where $n = II$ (see fig. 5a). Such a behaviour is very unusual since the system selects a mode of oscillation with larger spatial structures as the velocity increases.

In classical configurations, due to the boundary conditions on the jet nozzle and on the rigid impingement obstacle, selection of the wavelength occurs and consequently selection of the frequency. The selected frequency allows a fairly constant value of the Strouhal number $St = \frac{f.H}{U}$ to be kept whatever the wavelength. Jumps from one mode to another of higher frequency are observed as the impinging distance H is increased [2, 6]. It is commonly accepted in the literature that these jumps are due to some qualitative condition imposing the wavelength to be of the same order of the nozzle width d. It has also been observed that the propagation celerity of all modes is constant around $U/2$ [18]. As a consequence, for a given mode, the frequency linearly increases with the jet velocity. The slope of each linear evolution $f(U)$ is more pronounced as the Strouhal number plateau increases at each modal transition (see fig. 5b). The diagrams in fig. 5b show the main particular features of the presented jet instability. The central feature is a bounded evolution of the oscillation frequency between 3 Hz and 5 Hz. As the frequency increases linearly with U, when f reaches a value close to the resonance frequency a decreasing frequency jump occurs and a mode with larger wavelength is selected. Such a behaviour is at the moment unexplainable, but has to be related to the particular nature of the flexible boundary condition on the impinged surface.

Despite the weak deformations, the flow dynamics are strongly coupled to the free-surface characteristics. The system constituted by the jet and the deforming surface undergoes a pressure feedback loop resulting in a resonant oscillation. Classical theories [4] are unable to predict this unexpected response since the dynamics of the water/air free surface is absent from the pressure feedback on the inlet jet velocity profile. In the case of the submerged fountain, if the inlet velocity is further increased, a second instability develops (denoted as free surface instability in fig. 5a). Indeed, conversion of kinetic energy into potential energy makes the bump located at the free surface increase in height (10–20 mm). This situation becomes unstable and, consequently, the bump breaks laterally inducing periodic global oscillations of the water cavity. This secondary instability is related to large deformations of the free surface and gravity wave propagation. Frequency oscillation is roughly constant (2 Hz) and easily distinguishable from jet meandering in all the spectra. This kind of oscillation is related to the liquid column instability which may occur through the connecting flow beneath the lower edge of the cavity [10, 11]. Both instabilities coexist around the secondary threshold. As U is increased, only the free-surface instability subsists. Large-scale global oscillation of the water cavity imposes a bent shape on the jet (without an apparent spatial modulation). Studies of this secondary instability have been proposed by [10, 11] in a plane configuration and by [12] in an axisymmetric geometry. Future studies will be devoted to characterizing the influence of the interfacial parameters and to a more detailed analysis of the secondary instability.

* * *

The authors are grateful to C. Veit for his technical support with the design and the construction of the experimental device.

REFERENCES

[1] Sondhaus C., *Ann. Phys. (Leipzig)*, **91** (1854) 214.
[2] Rockwell D. and Naudascher E., *Ann. Rev. Fluid Mech.*, **11** (1979) 67.
[3] Sato H., *J. Fluid Mech.*, **7** (1959) 53.
[4] Crighton D. G., *J. Fluid Mech.*, **234** (1992) 361.
[5] Ho C. M. and Nosseir N. S., *J. Fluid Mech.*, **105** (1981) 119.
[6] Chanaud R. C. and Powell A., *J. Acoust. Soc. Am.*, **37** (1965) 902.
[7] Taylor G. I., *Proceedings of the 12th International Congress on Applied Mechanics, Stanford, 1968* (Springer) 1969, p. 382.
[8] Rockwell D. and Naudascher E., *Trans. ASME J. Fluids Eng.*, **100** (1978) 152.
[9] Friedman P. and Katz J., *Phys. Fluids*, **11** (1999) 2598.
[10] Maurel A., Cremer S. and Jenffer P., *Europhys. Lett.*, **39** (1997) 503.
[11] Madarame H. and Iida M., *JSME Int. J.*, **41** (1998) 610.
[12] Houard S., Daviaud F. and Bergé P., *Physica D*, **99** (1996) 318.
[13] Banks R. B. and Bhavamai A., *J. Fluid Mech.*, **23** (1965) 229.
[14] Rosler R. S. and Stewart G. H., *J. Fluid Mech.*, **31** (1968) 163.
[15] Yarin A. L. and Tchavdarov B., *J. Fluid Mech.*, **307** (1996) 85.
[16] Cruickshank J. O. and Munson B. R., *J. Fluid Mech.*, **113** (1981) 221.
[17] Brown G. B., *Proc. Phys. Soc. (London)*, **49** (1937) 493.
[18] Maurel A., Ern P., Zielinska B. J. A. and Weisfreid J. E., *Phys. Rev. E*, **54** (1996) 3643.